Article

Neuron

Synaptotagmin-7-Mediated Asynchronous Release Boosts High-Fidelity Synchronous Transmission at a Central Synapse

Highlights

- Syt7 KO does not alter fast release or short-term plasticity of calyx synapses
- Syt7 mediates a slow release phase in calyx synapses during prolonged Ca^{2+} influx
- Syt7-mediated asynchronous release produces a basal current during spike trains
- Asynchronous release during spike trains enables high-fidelity spike transmission

Authors

Fujun Luo, Thomas C. Südhof

Correspondence

fluo@stanford.edu (F.L.),
tcs1@stanford.edu (T.C.S.)

In Brief

Luo and Südhof demonstrate that synaptotagmin-7-mediated asynchronous release boosts fast synchronous transmission during high-frequency spike trains at the calyx synapse, thus expanding the computational role of asynchronous release to enable rapid information transfer at a fast central synapse.

Luo & Südhof, 2017, Neuron *94*, 826–839
May 17, 2017 © 2017 Elsevier Inc.
http://dx.doi.org/10.1016/j.neuron.2017.04.020

CellPress

CellPress

Neuron
Article

Synaptotagmin-7-Mediated Asynchronous Release Boosts High-Fidelity Synchronous Transmission at a Central Synapse

Fujun Luo[1,2,*] and Thomas C. Südhof[1,2,3,*]
[1]Department of Molecular and Cellular Physiology, Stanford University, Stanford, CA 94304-5453, USA
[2]Howard Hughes Medical Institute
[3]Lead Contact
*Correspondence: fluo@stanford.edu (F.L.), tcs1@stanford.edu (T.C.S.)
http://dx.doi.org/10.1016/j.neuron.2017.04.020

SUMMARY

Synchronous release triggered by Ca^{2+} binding to synaptotagmin-1, -2, or -9 is thought to drive fast synaptic transmission, whereas asynchronous release induced by Ca^{2+} binding to synaptotagmin-7 is thought to produce delayed synaptic signaling, enabling prolonged synaptic computations. However, it is unknown whether synaptotagmin-7-dependent asynchronous release performs a physiological function at fast synapses lacking a prolonged signaling mode, such as the calyx of Held synapse. Here, we show at the calyx synapse that synaptotagmin-7-dependent asynchronous release indeed does not produce a prolonged synaptic signal after a stimulus train and does not contribute to short-term plasticity, but induces a steady-state, asynchronous postsynaptic current during stimulus trains. This steady-state postsynaptic current does not increase overall synaptic transmission but instead sustains reliable generation of postsynaptic spikes that are precisely time locked to presynaptic spikes. Thus, asynchronous release surprisingly functions, at least at some synapses, to sustain high-fidelity neurotransmission driven by synchronous release during high-frequency stimulus trains.

INTRODUCTION

The timing and efficiency of neurotransmission critically depend on the kinetics and probability of neurotransmitter release (Stevens, 2003; Trussell, 1999). In all synapses, an action potential stimulates fast synchronous neurotransmitter release within less than a millisecond. Synchronous release is triggered by Ca^{2+} binding to synaptotagmin-1 (Syt1), -2 (Syt2), or -9 (Syt9), which serve as Ca^{2+} sensors for fast release with slightly different kinetic properties (Xu et al., 2007). At many synapses, action potentials activate a second asynchronous form of release that is not tightly coupled to the action potential (Goda and Stevens, 1994). Asynchronous release is largely mediated by Ca^{2+} binding to synaptotagmin-7 (Syt7), which exhibits a higher Ca^{2+} affinity than Syt1, Syt2, and Syt9 (Wen et al., 2010; Bacaj et al., 2013; Sugita et al., 2002). Synchronous and asynchronous release compete with each other physiologically, with synchronous release accounting for the vast amount of transmission (Hagler and Goda, 2001; Otsu et al., 2004). In addition to their synaptic roles as Ca^{2+} sensors for synchronous and asynchronous release, Syt1 and Syt7 are Ca^{2+} sensors for neuroendocrine exocytosis, for which Syt1 again mediates a faster and Syt7 a slower phase (Schonn et al., 2008; Sugita et al., 2001). Finally, deletions of Syt7 in some synapses cause a change in short-term plasticity, which has been interpreted to indicate that Syt7 is a Ca^{2+} sensor for such plasticity (Jackman et al., 2016).

The probability of synchronous neurotransmitter release varies greatly among synapses, producing large differences in the reliability and plasticity of synaptic transmission. Similarly, great heterogeneity of asynchronous release was observed among synapses. At many synapses, asynchronous release contributes a delayed signal that continues after a burst or train of action potentials (Maximov and Südhof, 2005; Luo et al., 2015). In the most extreme case, specific subclasses of GABAergic interneurons, such as CCK neurons, form synapses mediating prolonged synaptic computations at which delayed asynchronous release predominates under physiological conditions (Best and Regehr, 2009; Daw et al., 2009, 2010; Hefft and Jonas, 2005; Iremonger and Bains, 2007). On the other hand, at synapses specialized for fast information transfer, such as the calyx of Held, asynchronous release is completely occluded by synchronous release, and no delayed synaptic signal is detectable (Sun et al., 2007). Here, an asynchronous component can be exposed upon deletion of fast synaptotagmin Ca^{2+} sensors but performs no obvious physiological function (e.g., see Geppert et al., 1994; Yoshihara and Littleton, 2002; Sun et al., 2007; Xu et al., 2012; Bacaj et al., 2013).

Thus, the nature and physiological significance of asynchronous release in synapses remain incompletely understood (Walter et al., 2011; Crawford and Kavalali, 2015; Kaeser and Regehr, 2014; Evstratova et al., 2014). Although the properties of synapses in which asynchronous release predominates suggest a function in extending the synaptic signaling time window, the function of asynchronous release in synapses that do not exhibit delayed asynchronous release remains unknown. Interestingly, synchronous and asynchronous release are evolutionarily

conserved (Yoshihara and Littleton, 2002) and differentially regulated (Daw et al., 2009, 2010), arguing for a fundamental role. As a result, two major questions arise. First, given the well-established roles of asynchronous release in delayed synaptic signaling at some synapses and of Syt7 as a Ca^{2+} sensor for asynchronous release, does asynchronous release exist in neurons that exhibit no delayed synaptic signaling, and what is the function of Syt7 in these neurons? Either Syt7 has to perform a different function in these neurons or the physiological role of asynchronous release at these synapses is different from that currently envisioned. Second, does Syt7 perform an independent second function in presynaptic terminals different from its role as a Ca^{2+} sensor for asynchronous release, namely as a Ca^{2+} sensor for short-term facilitation? Alternatively, is the proposed second role of Syt7 as a Ca^{2+} sensor for short-term plasticity based on an interpretation of experimental results that could also be explained by a role of Syt7 as a Ca^{2+} sensor for asynchronous release?

To address these questions, we here examined the role of Syt7 at the calyx of Held synapse, which reliably and precisely mediates transmission of presynaptic action potentials at rates of >100 Hz. Since calyx synapses exhibit no delayed asynchronous signals, but feature prominent short-term synaptic plasticity, they are ideally suited for testing these questions. Our data show that Syt7 indeed mediates asynchronous release at the calyx synapse but that this asynchronous release unexpectedly manifests as a basal postsynaptic current during and not after a stimulus train. This basal current functions to boost synchronous postsynaptic spike generation. Short-term synaptic plasticity was unaffected by deletion of Syt7 in wild-type synapses but blocked the synaptic facilitation that results from deletion of Syt2 as the major fast Ca^{2+} sensor at the calyx synapse, conferring onto Syt7 the properties of an apparent Ca^{2+} sensor for short-term synaptic plasticity, even though it just acts as a Ca^{2+} sensor for asynchronous release. We propose that a major function of asynchronous release, at least at fast synapses, is to operate concurrently with synchronous release to sustain precise synaptic transmission during bursts and trains of action potentials and that in addition, asynchronous release acts to allow prolonged synaptic signaling at some synapses, and furthermore contribute to short-term synaptic plasticity at these or other synapses.

RESULTS

To examine the precise role of Syt7 in neurotransmitter release and information coding at a synapse that is specialized for fast and accurate synaptic transmission, we focused on the calyx of Held synapse in the auditory system. This glutamatergic synapse accurately transmits high-frequency spikes at more than 100 Hz, as required for its role in sound localization in which binaural inputs differing only in milliseconds are compared (Baydyuk et al., 2016; Takahashi, 2015; Trussell, 1999; Wang and Augustine, 2015). In the calyx synapse, a large presynaptic terminal forms hundreds of synaptic junctions on the soma of a postsynaptic neuron in the medial nucleus of the trapezoid body (MNTB). The structure of calyx synapses enables patch clamping of both the pre- and the postsynaptic compartments and allows synaptic recordings at an unprecedented precision (Borst and Sakmann, 1996; Forsythe, 1994), rendering this synapse ideal for high-resolution analyses of synaptic transmission.

Syt7 Is Not Required for Basal Synaptic Transmission or Short-Term Plasticity

We first characterized the effect of the Syt7 KO on basal synaptic transmission at the calyx synapse. We induced presynaptic action potentials by afferent fiber stimulation and recorded excitatory postsynaptic currents (EPSCs) in MNTB neurons. We observed no significant difference between Syt7 KO and littermate control mice in the frequency and amplitude of spontaneous EPSCs (sEPSCs, Figure 1A) or in the amplitude of EPSCs evoked by isolated action potentials (Figure 1B). These results confirm that Syt7 is not on its own required for clamping spontaneous mini release or for mediating fast Ca^{2+}-triggered release, consistent with previous studies on other synapses (Wen et al., 2010; Bacaj et al., 2013; Luo et al., 2015; Jackman et al., 2016).

A recent report showed that Syt7-deficient central synapses exhibit a decrease in short-term synaptic facilitation, suggesting a novel function for Syt7 as a Ca^{2+} sensor for short-term plasticity (Jackman et al., 2016). Such a function implies a different role for Syt7 than previously envisioned, a role that may have been missed because previous studies only examined Syt7 in cultured neurons and not in acute slices (Jackman et al., 2016). However, the decrease in synaptic facilitation by the Syt7 KO could also be interpreted as a direct consequence of the loss of Syt7-mediated asynchronous release, consistent with previous studies (Wen et al., 2010; Bacaj et al., 2013).

To differentiate between these two hypotheses, we examined the impact of the Syt7 KO on short-term synaptic plasticity at the calyx synapse. Under standard recording conditions, the calyx synapse has a relatively high release probability; as a result, EPSCs elicited by two closely spaced action potentials exhibited strong paired-pulse depression (Figure 1C). The Syt7 KO had no effect on this form of short-term plasticity, suggesting that Syt7 is not involved in setting the release probability at the calyx synapse or in short-term plasticity (Figure 1C). However, the synaptic depression at the calyx under standard recording conditions using 2 mM extracellular Ca^{2+} may have occluded a potential role for Syt7 in synaptic facilitation (Lorteije et al., 2009). Lowering extracellular Ca^{2+} to 0.6 mM induced prominent synaptic facilitation at the calyx synapse, but again the Syt7 KO caused no change (Figure 1D). We also tested synaptic facilitation in response to 100 Hz stimulus trains in 0.6 mM Ca^{2+}, but again found no change (Figure 1E). Together, these results show that Syt7 is not required for short-term facilitation at the calyx synapse under physiological conditions.

Generation of Syt2 Conditional KO Mice and Syt27 Double KO Mice

In cultured hippocampal neurons, Syt7 provides only a minor contribution to Ca^{2+}-triggered neurotransmitter release when Syt1 as the fast Ca^{2+} sensor is present because Syt1 outcompetes Syt7, owing to its faster Ca^{2+}-binding properties (Maximov and Südhof, 2005; Maximov et al., 2008; Bacaj et al., 2013). A prominent role for Syt7 in release is uncovered, however, when Syt1 is deleted, prompting us to test whether the same applies

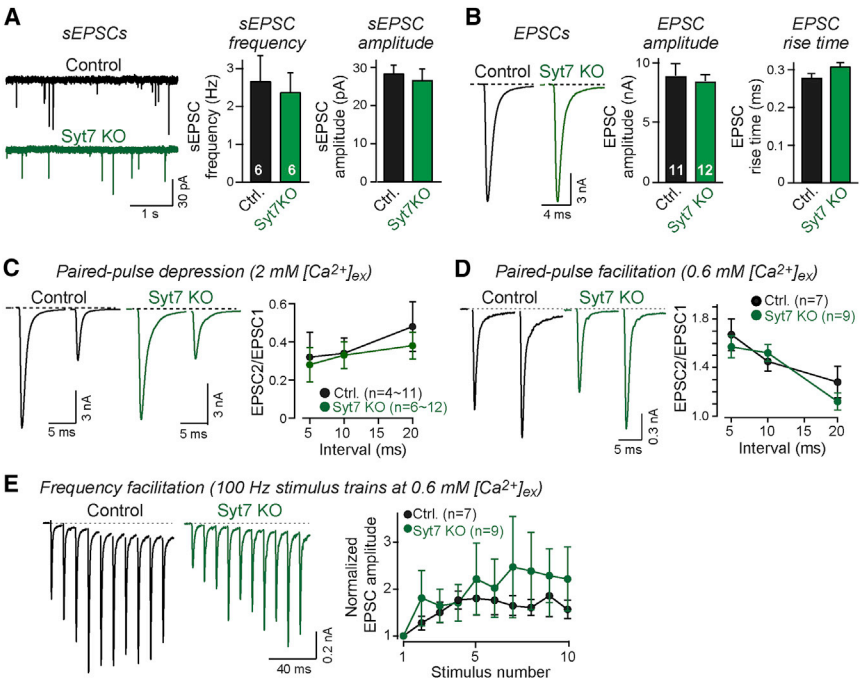

Figure 1. Syt7 Is Not Required for Basal Synaptic Transmission or Short-Term Synaptic Plasticity at the Calyx of Held Synapse

(A) Example traces and summary graphs of the frequency and amplitude of spontaneous EPSCs (sEPSCs) recorded from patched MNTB neurons in acute brainstem slices from littermate control (Ctrl.) and Syt7 KO mice at P11–P14 under standard conditions in 2 mM extracellular Ca^{2+}.

(B) Example traces and summary graphs of the amplitude and rise time (20%–80%) of EPSCs evoked by fiber stimulation recorded from MNTB neurons under standard conditions.

(C) Example traces of EPSCs induced by two closely spaced stimuli (left) and summary graph of the ratio of peak amplitudes of the two closely spaced EPSCs plotted as a function of interstimulus intervals (right). Recordings were from MNTB neurons under standard conditions with 2 mM extracellular Ca^{2+}.

(D) Same as (C) but recorded in 0.6 mM extracellular Ca^{2+}.

(E) Example traces of EPSCs induced by a 100 Hz stimulus train (left) and summary graph of the normalized peak EPSC amplitude during the train (right), recorded in 0.6 mM extracellular Ca^{2+}.

Data are means ± SEM. Number of cells (from at least three mice per group) analyzed are indicated in the bars (A and B) or shown in the graphs (C–E); no statistically significant differences were observed as assessed by Student's t test (A and B) or one-way *ANOVA* (C–E).

to calyx synapses, which exhibit much less asynchronous release in the wild-type condition than hippocampal synapses (Sun et al., 2007).

To address this question, we generated conditional KO (cKO) mice of Syt2, the major Ca^{2+} sensor for fast synchronous release at the calyx of Held synapse (Figures 2A and 2B; Pang et al., 2006a, 2006b; Sun et al., 2007; Kochubey and Schneggenburger, 2011). We then crossed Syt2 cKO mice with mice expressing Cre-recombinase under control of the parvalbumin promoter (PV-Cre mice), which allows deletion of Syt2 in presynaptic calyx neurons because parvalbumin is expressed early postnatally (Felmy and Schneggenburger, 2004; Zhang et al., 2016). Adolescent PV-Cre/Syt2 cKO mice were indistinguishable in size and survival rates from control littermates, in contrast to the severe growth defect observed in Syt2 constitutive KO mice (Pang et al., 2006a, 2006b; Sun et al., 2007). To confirm that expression of Syt2 was fully deleted from the calyx of Held in PV-Cre/Syt2 cKO mice, we stained brainstem sections with Syt2-specific antibodies. By P11, Syt2 was undetectable at the calyx of Held in PV-Cre/Syt2 cKO mice but robustly observed in littermate control mice (Figure 2B).

Syt7 Clamps Spontaneous Mini Release in Syt2-Deficient Synapses but Makes No Contribution to Synchronous Release

Synaptic recordings in PV-Cre/Syt2 cKO mice revealed that the Syt2 deletion caused an ~8-fold increase in the frequency of miniature EPSCs (mEPSCs) and a >10-fold increase in the frequency of spontaneous EPSCs (sEPSCs) (Figures 2C–2F). Moreover, the Syt2 deletion produced a >10-fold decrease in the amplitude of EPSCs evoked by isolated action potentials (Figures 2G and 2H). As described previously, Syt2-deficient calyx synapses exhibited residual fast synchronous release (<5% of control), consistent with the developmental coexpression of Syt1 in all Syt2-expressing neurons in young mice (Pang et al., 2006a, 2006b). This coexpression declines with the maturation of mice (Pang et al., 2006a, 2006b; Kochubey et al., 2016). Probably because Syt1 acts slower in synchronous release than Syt2 (Xu et al., 2007), the Syt2 deletion caused an increase in EPSC rise times (Figures 2G and 2H). Overall, the phenotype of the Syt2 cKO mice was thus identical to that described previously for Syt2 constitutive KO mice (Sun et al., 2007; Kochubey and Schneggenburger, 2011).

We next compared spontaneous and evoked release between Syt2-deficient and Syt2/7 double deficient calyx synapses (Syt2/7). Strikingly, we found that the additional deletion of Syt7 in Syt2-deficient calyx synapses further increased the frequency of mEPSCs and sEPSCs, that was already enhanced by the Syt2 deletion, to more than 40 Hz (Figures 2C–2F). Because these mEPSC and sEPSC frequencies are beyond the resolution of our measurements, they are likely an underestimate, suggesting that Syt7 significantly contributes to clamping spontaneous release when Syt2 is absent.

However, the additional Syt7 deletion caused no further decrease in Syt2-deficient calyx synapses in evoked EPSC amplitude or synchronous neurotransmitter release, as measured via the amplitude and total synaptic charge transfer of EPSCs evoked by isolated action potentials (Figures 2G and 2H). Moreover, the

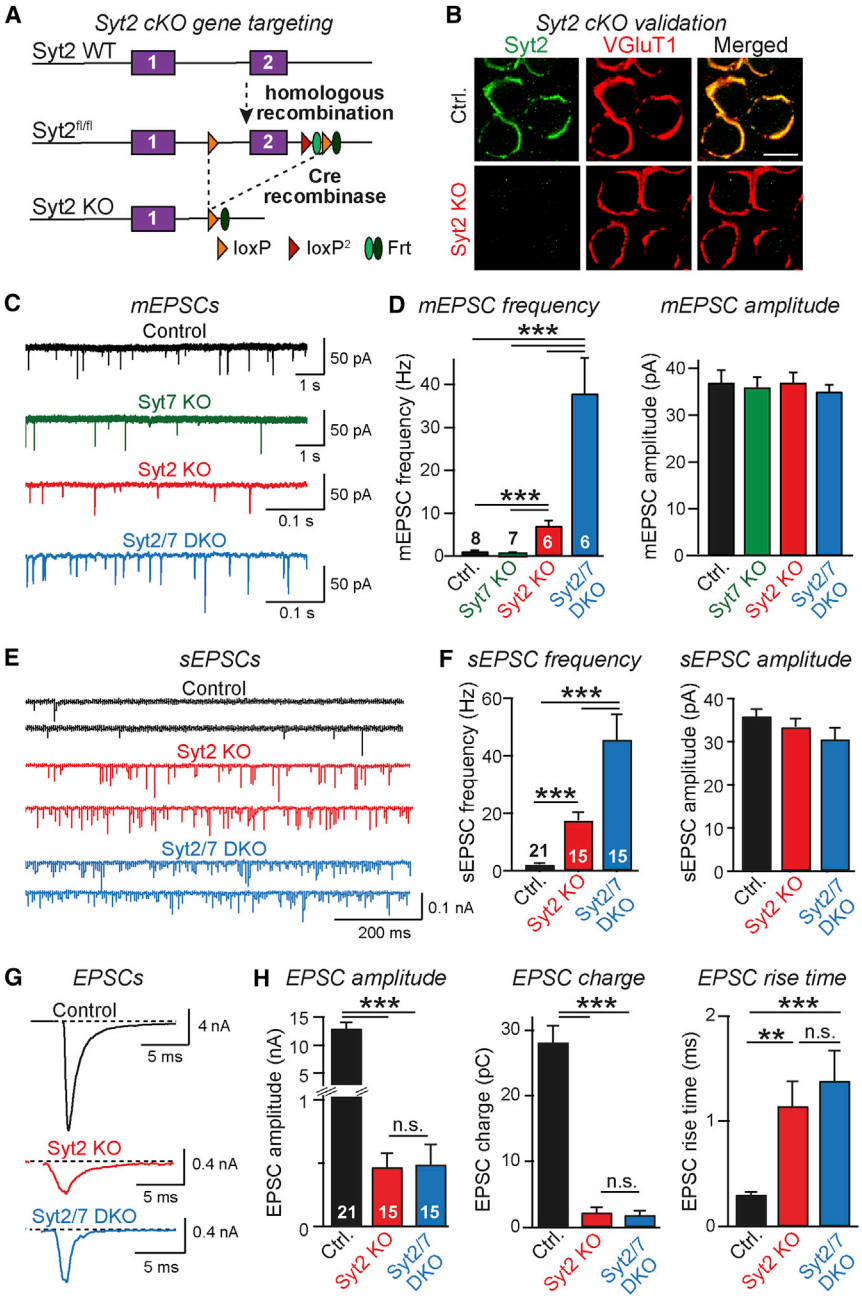

Figure 2. The Increase in Spontaneous Release in Syt2 KO Neurons Is Enhanced by the Additional KO of Syt7, Whereas the Decrease in Synchronous Release in Syt2 KO Neurons Is Not Enhanced

(A) Strategy for generating Syt2 cKO mice. Exon 2 encoding the Syt2 transmembrane region was flanked by loxP sites using homologous recombination in embryonic stem cells, allowing Cre-recombinase-mediated excision of exon 2 and conditional deletion of Syt2 expression (see Figures S1A–S1C).

(B) Validation of Syt2 cKO mice by crossing Syt2 cKO mice with Pv-Cre transgenic mice that mediated deletion of floxed genes in calyx synapses (Zhang et al., 2016). Brainstem sections from control and Syt2 cKO/Pv-Cre mice were labeled with antibodies to Syt2 and VGluT1 as indicated. Scale bar, 20 μm.

(C) Representative traces of mEPSCs recorded in MNTB neurons in acute brainstem slices from littermate control, Syt2 KO, Syt7 KO, and Syt2/7 DKO mice at P11–P14 in the presence of 1 μM tetrodotoxin. Note that traces are shown at different scales to visualize mEPSCs in Syt2 KO and Syt2/7 DKO samples.

(D) Summary graphs of the mEPSC frequency and amplitude.

(E) Representative traces of spontaneous sEPSCs recorded in MNTB neurons in acute brainstem slices from littermate control, Syt2 KO, and Syt2/7 DKO mice at P11–P14 under standard conditions.

(F) Summary graphs of the sEPSC frequency and amplitude.

(G) Representative traces of EPSCs recorded in MNTB neurons in acute brainstem slices from littermate control, Syt2 KO, and Syt2/7 DKO mice. EPSCs were evoked by isolated action potentials induced by extracellular fiber stimulation. Note that significant synchronous release remains in Syt2 KO and Syt2/7 DKO synapses due to the continued presence of Syt1 (Pang et al., 2006b).

(H) Summary graphs of the EPSC amplitude, charge transfer, and rise times.

Data are means ± SEM. Number of cells (from at least three mice per group) analyzed are indicated in the bars (D, F, and H); statistical significance was assessed by one-way *ANOVA* with Tukey's post hoc test (**p < 0.01; ***p < 0.001).

Syt2/7 double deletion did not induce a further increase in EPSC rise times. Thus, Syt7 does not significantly contribute to synchronous release at the calyx synapse but acts as a "backup" clamp for spontaneous release in Syt2-deficient synapses.

Capacitance Measurements Uncover a Direct Role for Syt7 in Ca^{2+}-Evoked Neurotransmitter Release

Our results up to this point revealed only a single effect of Syt7 deletions on release: aggravating the already dramatic increase in spontaneous release induced by the Syt2 KO, a phenotype that was not detected when Syt7 was deleted in Syt2-expressing synapses. These results raise the question of whether Syt7 performs any role at all in evoked exocytosis at calyx synapses. Is it possible that Syt7 is an evolutionary relict that has become superfluous in a fast-transmitting synapse like the calyx of Held? This question is particularly pertinent because quantifications revealed that delayed release (which is observed after a high-frequency stimulus train in many synapses and thought to be due to asynchronous release) is negligible at calyx synapses, accounting for only ~0.1% of the total release during the train (Figures S2A–S2D).

To test the question of whether Syt7 plays any role at the calyx synapse, we examined Ca^{2+}-triggered presynaptic exocytosis in calyx terminals from littermate control and PV/Cre-Syt2 cKO

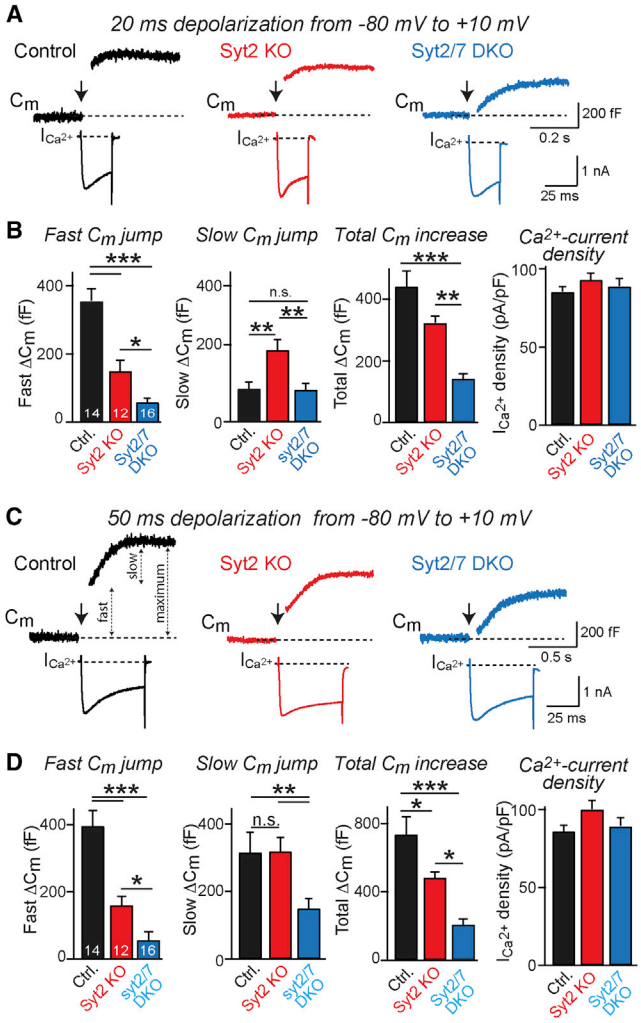

Figure 3. Capacitance Measurements Reveal Major Contributions of Both Syt2 and Syt7 to Ca^{2+}-Triggered Exocytosis in Presynaptic Calyx Terminals

(A) Example traces of simultaneous measurements of the presynaptic capacitance (C_m) and Ca^{2+} currents in patched calyx terminals from littermate control, Syt2 KO, and Syt2/7 DKO mice. Increases in capacitance due to synaptic vesicle exocytosis and Ca^{2+} currents were induced by a 20 ms step depolarization from −80 mV to +10 mV.

(B) Summary graphs of the fast and slow components and the total of the depolarization-induced capacitance jump as well as the Ca^{2+} current density measured as described in (A). The fast and slow capacitance jump components were calculated as the capacitance increases induced during or after the depolarization, respectively.

(C and D) Same as (A) and (B), except that depolarization periods were 50 ms instead of 20 ms.

Data are means ± SEM. Number of cells (from at least three mice per group) analyzed are indicated in the bars (B and D); statistical significance was assessed by one-way *ANOVA* with Tukey's post hoc test (*$p < 0.05$; **$p < 0.01$; ***$p < 0.001$). For additional data, see Figures S2E–S2H.

mice without and with the Syt7 KO using patch-clamp capacitance measurements that directly monitor exocytosis. We depolarized patched terminals from a holding potential of −80 mV to +10 mV to induce maximal Ca^{2+} influx and recorded the total nerve-terminal capacitance change induced by the Ca^{2+} influx (Lindau and Neher, 1988; Sun and Wu, 2001). In order to grasp any possible effect of the Syt7 deletion, we used both short- (20 ms) and long-period depolarizations (50 ms; Figures 3A–3D). Moreover, to ensure that the synaptotagmin deletions had no effect on Ca^{2+} channels, we simultaneously measured depolarization-evoked Ca^{2+} currents (Figures 3A–3D and S2E). Control experiments confirmed that the depolarizations did not cause major changes in the intrinsic membrane or series resistance (Figure S2F).

In control terminals, 20 ms and 50 ms depolarizations induced two phases of capacitance change: a large fast capacitance jump, followed by a smaller, slower capacitance increase that continues after the depolarizations, with the fast phase accounting for the majority (>80%) of the total capacitance change (Figures 3A–3D). Deletion of Syt2 strongly reduced the fast capacitance jump (>60%) but either slightly increased the slower phase (for the 20 ms depolarization) or left the slower phase unaffected (for the 50 ms depolarization), consistent with the function of Syt2 as a Ca^{2+} sensor for fast synchronous synaptic vesicle exocytosis. Additional deletion of Syt7 in Syt2 cKO synapses produced a significant further reduction in the fast capacitance jump to a total decrease of 85%–90% and either had no significant effect on the slow phase of capacitance increase (for the 20 ms depolarizations) or also decreased the slow phase (for the 50 ms depolarizations; Figures 3A–3D), suggesting that Syt7 contributes a major component to overall Ca^{2+}-induced exocytosis. None of the genetic manipulations altered the starting capacitance of calyx terminals or the density of depolarization-induced Ca^{2+} currents (Figures 3A–3D, S2G, and S2H). These data demonstrate that the total exocytosis induced by prolonged presynaptic depolarization, as opposed to exocytosis triggered by single action potentials, contains a significant Syt7-dependent component, suggesting that Syt7 is, after all, a major contributor to the Ca^{2+}-triggering machinery for exocytosis at calyx synapses at least when Syt2 is deleted.

Syt7 Mediates Asychronous Release during High-Frequency Stimulus Trains

The unexpectedly large effect of the Syt7 deletion on total vesicle exocytosis induced by 20–50 ms depolarizations of Syt2-deficient nerve terminals, compared to the lack of an effect of the Syt7 deletion on release in Syt2-deficient synapses induced by <2 ms depolarizations during isolated action potentials, suggests that Syt7-dependent exocytosis may initiate in Syt2-deficient synapses during the 2–20 ms time window. Thus, we asked whether the Syt7 deletion might affect release in Syt2-deficient calyx synapses stimulated by action potential trains that extend beyond this time window.

In response to presynaptic 100 Hz, 0.5 s action potential trains, control calyx synapses exhibited large initial EPSCs (>10 nA) that rapidly depressed during the train but remained synchronous throughout (Figure 4A). The Syt2 KO caused a large decrease (>95%) in EPSC amplitudes, as expected, but a lesser decrease (~40%) in the total amount of release during the train, as measured by the synaptic charge transfer (Figures 4A–4D and S3). Moreover, the Syt2 KO resulted in a marked initial shift

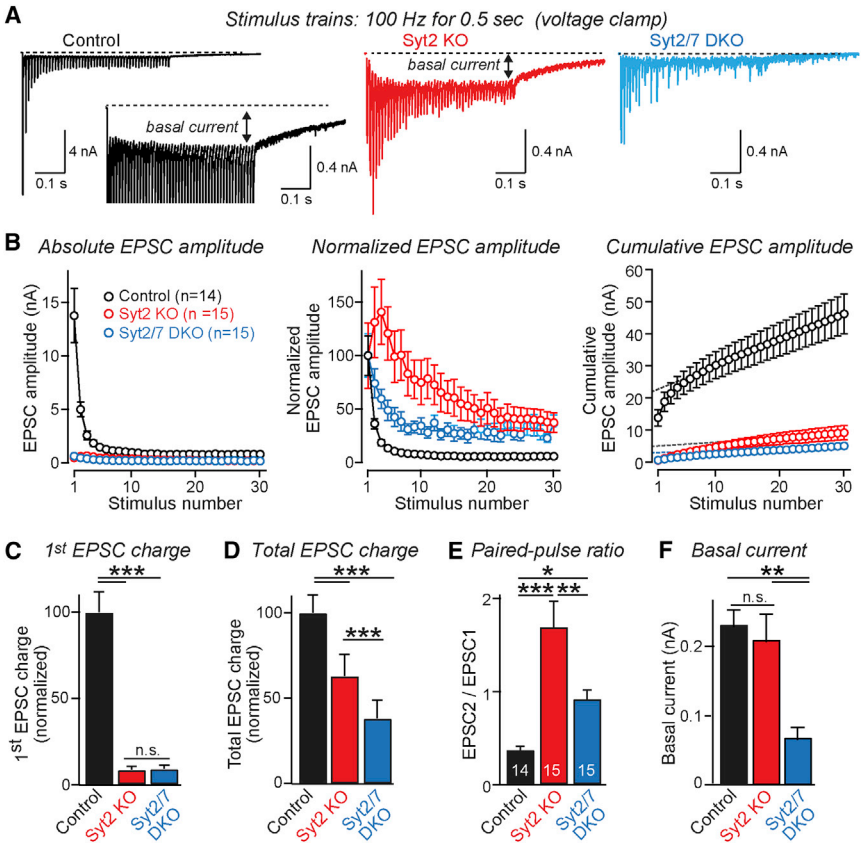

Figure 4. High-Frequency Stimulus Trains Induce a Sustained Basal Asynchronous EPSC in Wild-Type Calyx Synapses that Requires Syt7 but Not Syt2

(A) Representative traces of EPSCs evoked by extracellular fiber stimulation at high frequency (100 Hz for 0.5 s) in acute brainstem slices from littermate control, Syt2 KO, and Syt2/7 DKO mice at P11–P14. Expanded control trace illustrates the Syt7-dependent basal asynchronous current, on top of which Syt2-dependent synchronous EPSCs ride. Note that, as for isolated stimuli, the Syt2/7 DKO only abolishes ~90% of synchronous release during repeated stimuli because low levels of Syt1 remain in the Syt2/7 DKO and mediate the residual synchronous release.

(B) Summary graphs of the absolute, normalized, and cumulative EPSC amplitudes. The gray dotted lines in the cumulative EPSC plot illustrate linear regression fits used to estimate the cumulative EPSC amplitude by back-extrapolation to time zero, which corrects for vesicle replenishment during the train.

(C and D) Summary graphs of the synaptic charge transfer during the 1st EPSC (C) or the entire trains (D), normalized to control.

(E) Summary graph of the paired-pulse (10 ms interval) ratio of the peak amplitudes of the 2nd and 1st EPSCs. Note that when the Syt2 KO decreases synchronous Ca^{2+} sensor activity, the asynchronous Ca^{2+} sensor Syt7 appears to become essential for synaptic facilitation.

(F) Summary graph of the basal current amplitudes, measured as the difference between the sustained currents reached during the train and the baseline (dotted line).

Data are means ± SEM. Number of cells (from at least three mice per group) analyzed are shown in the graph (B) or indicated in the bars (E); statistical significance was assessed by one-way *ANOVA* with Tukey's post hoc test (*p < 0.05; **p < 0.01; ***p < 0.001). For additional data, see Figures S3–S5.

in short-term plasticity from synaptic depression to facilitation (Figures 4A, 4B, and 4E). These results are consistent with a decreased release probability by ablation of Syt2 as the major Ca^{2+} sensor for fast synchronous exocytosis, with the remaining Syt1 mediating the residual synchronous release (Sun et al., 2007; Kochubey et al., 2016).

Deletion of Syt7 in addition to Syt2 did not have a major effect on EPSC amplitudes but induced a further, significant 20% decline in total synaptic charge transfer (Figures 4A–4D). This result confirms the capacitance measurements (Figure 3), showing that additional deletion of Syt7 in Syt2-deficient synapses causes a large decrease in overall release elicited by prolonged stimulation. Strikingly, the Syt7 KO also reversed the initial synaptic facilitation observed in Syt2-deficient synapses, as best appreciated from a quantification of the initial paired-pulse facilitation (Figure 4E). However, neither the Sy2 KO nor the additional deletion of Syt7 in Syt2 KO synapses had a significant effect on the delayed EPSC after the stimulus train (Figures S2A–S2D). Thus, only when Syt2 is deleted from calyx synapses does Syt7 behave like an apparent Ca^{2+} sensor for short-term synaptic facilitation, suggesting that the relative ratio of fast (Syt1 and Syt2 in the case of the calyx) to slow Ca^{2+} sensors (Syt7) controls short-term synaptic plasticity.

Since the Syt7 KO decreased the total release induced by a stimulus train in Syt2-deficient calyx synapses without changing the amplitude of synchronous release, the contribution of Syt7 must be comprised of an asynchronous component that is not manifested in the synchronous EPSCs. To test this hypothesis, we examined nonsynchronous EPSCs during the stimulus train. We observed that, during the train, the "baseline" of synchronous EPSCs was increased by a basal current (Figure 4A). This basal current was similar in control and Syt2-deficient synapses but greatly reduced in Syt2/7 double deficient synapses. Quantification revealed that the basal current was unchanged by the Syt2 deletion but decreased >70% by the additional Syt7 deletion, which accounts for the decrease in total synaptic charge transfer induced by the Syt7 deletion on top of the Syt2 deletion (Figures 4A and 4D). These phenotypes were similarly observed in a comparison of control with Syt2/7 double KO synapses with experiments that included γ-DGG to avoid receptor saturation (Figure S4). Consistent with the identification of the basal current as a result of asynchronous release during the train, application of EGTA-AM to calyx synapses had no effect on synchronous EPSC amplitudes but greatly impaired the basal current during high-frequency stimulus trains (Figure S5), as would be expected for asynchronous release (Maximov and Südhof, 2005). Viewed together, these results show that stimulus trains induce both synchronous and asynchronous release in calyx synapses and that both release forms contribute significantly to the total synaptic charge transfer but differentially

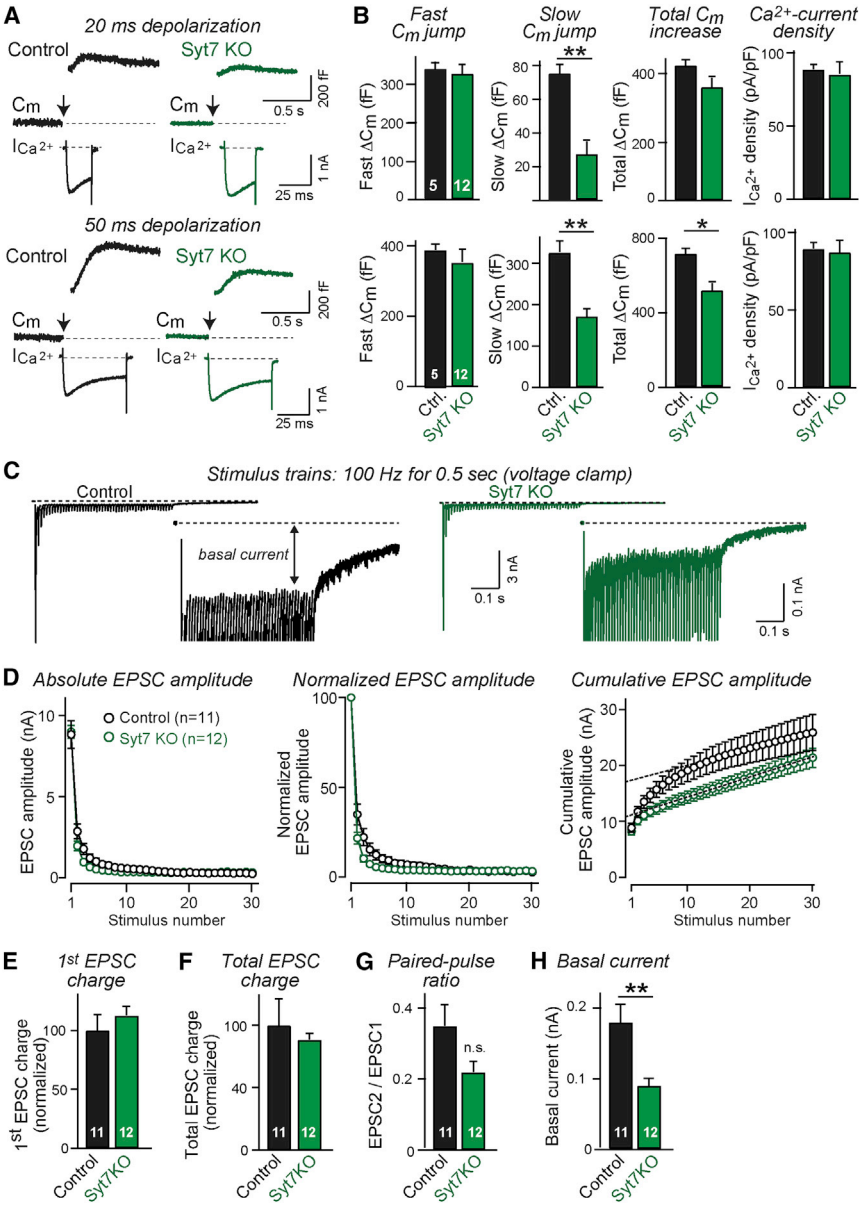

Figure 5. Syt7 Is Required for a Sustained Component of Exocytosis during Prolonged Presynaptic Depolarization that Manifests as an Asynchronous Basal Current during High-Frequency Stimulus Trains in Calyx Synapses

(A) Example traces of simultaneous measurements of the presynaptic capacitance (C_m) and Ca^{2+} currents in patched calyx terminals from littermate control and Syt7 KO mice. Synaptic vesicle exocytosis and Ca^{2+} currents were induced by step depolarizations from −80 mV to +10 mV lasting for 20 ms (top) or 50 ms (bottom).

(B) Summary graphs of the fast and slow capacitance jump components and the total of the depolarization-induced capacitance jump as well as the Ca^{2+} current density measured as described in (A), for 20 ms (top) and 50 ms (bottom) step depolarizations. The fast and slow capacitance jump components were calculated as the capacitance increases induced during or after the depolarization, respectively.

(C) Representative traces of EPSCs evoked by high-frequency trains of extracellular fiber stimulation (100 Hz for 0.5 s) in acute brainstem slices from littermate control, Syt2 KO, and Syt2/7 DKO mice at P11–P14. Expanded traces below full traces illustrate the basal asynchronous EPSC on which synchronous EPSCs ride. Note that Syt7 is selectively required for the basal asynchronous EPSC.

(D) Summary plots of the absolute, normalized, and cumulative EPSC amplitudes plotted against stimulus number. The gray dotted lines in the cumulative EPSC plot illustrate the linear regression fit used to estimate the cumulative EPSC amplitude by back-extrapolation to time zero, which corrects for vesicle replenishment during the train.

(E–H) Summary graphs of the normalized synaptic charge transfer during the 1st EPSC (E) or the entire trains (F), the paired-pulse (10 ms interval) ratio of the peak amplitudes of the 2nd and 1st EPSCs (G), and the basal current amplitudes (H), measured as the difference between the sustained currents reached during the train and the baseline (dotted line).

Data are means ± SEM. Number of cells (from at least three mice per group) analyzed are indicated in the bars (B and E–H) or shown in the graph (D); statistical significance was assessed by Student's t test (B and E–H; *$p < 0.05$; **$p < 0.01$). For additional data, see Figure S6.

require Syt2 (synchronous release) or Syt7 (asynchronous release).

Syt7 Makes a Physiological Contribution to Release at Calyx Synapses

Is the impairment in asynchronous release by the Syt7 deletion that we observed in Syt2-deficient calyx synapses induced by the Syt2 deletion, i.e., only observed in the absence of Syt2 similar to the unclamping of spontaneous release (Figures 2C–2F)? Or does this impairment reflect a Syt7 function that is physiologically relevant and also operates in the presence of Syt2? To address this question, we analyzed the effect of the Syt7 KO on exocytosis using presynaptic capacitance measurements (Figures 5A and 5B) and on the basal current induced by 100 Hz stimulus trains using postsynaptic recordings (Figures 5C–5H).

Presynaptic capacitance measurements revealed that the Syt7 KO on its own had no significant effect on the fast depolarization-induced capacitance jump but caused a large decrease of the slow capacitance jump and a corresponding decrease of the total capacitance jump (Figures 5A and 5B). No effect of the Syt7 KO on Ca^{2+} current density was detected. These results show that during prolonged depolarization, Syt7-triggered exocytosis makes a significant contribution to overall neurotransmitter release.

In the analysis of 100 Hz stimulus trains, we found that the Syt7 deletion, as expected, had no effect on the amplitude or

short-term plasticity of synchronous EPSCs (Figures 5C–5G and S6). Moreover, the Syt7 deletion did not decrease the total synaptic charge transfer induced by the stimulus train (Figure 5F). However, we observed that the Syt7 KO induced a highly significant decrease (~50%) in the basal current during the train (Figures 5C and 5H). As shown above, the basal current induced by stimulus trains is largely due to asynchronous release that does not directly trigger postsynaptic spikes time locked with action potentials. The Syt7-KO-induced decrease in basal current was not due to a decrease in the decay time constant of synchronous EPSCs, which was unchanged (Figure S6E). Viewed together, these data demonstrate that Syt7-dependent asynchronous release does, after all, have a physiological function at the calyx synapse, but an unexpected function: producing a baseline EPSC during a stimulus train without changing synchronous release.

Syt7-Mediated Asynchronous Release Supports Reliable Action Potential Firing

The fact that the sustained basal EPSC evoked during high-frequency train stimulation (which is selectively mediated by Syt7-dependent asynchronous release) contributes only a minor component to overall release under physiological conditions (Figure 5F) raises the critical question of whether Syt7-mediated asynchronous release has a physiological role at calyx synapses. Indeed, the general physiological function of asynchronous release, despite its wide presence, remains poorly understood, primarily because asynchronous release is always dwarfed by synchronous release and often only detectable under conditions in which synchronous release is impaired.

A major role proposed for asynchronous release is to prolong the signal-processing time window for postsynaptic cells, thereby providing tonic inhibition or excitation (Hefft and Jonas, 2005; Iremonger and Bains, 2007). However, prolonging signaling is unlikely to be important for many excitatory synapses, especially for fast, phase-locked relay synapses like the calyx of Held that exhibit only negligible delayed release (Figures S2A–S2D). As an alternative hypothesis, the basal postsynaptic current during high-frequency spike trains that is produced by asynchronous release at calyx synapses might paradoxically support synchronous synaptic transmission by sustaining membrane depolarization to a level closer to the spiking threshold.

To test this hypothesis, we measured postsynaptic spike patterns in response to presynaptic action potential trains using current-clamp recordings in calyx synapses from littermate control and Syt7 KO mice. As shown exemplarily for 100 Hz trains in Figures 6A and 6B, we monitored postsynaptic action potentials in response to trains of 50 presynaptic stimuli applied at frequencies of 20–200 Hz. In control mice, most presynaptic stimuli induced phase-locked postsynaptic action potentials throughout the train, consistent with in vivo recordings (Lorteije et al., 2009; Mc Laughlin et al., 2008); no extraneous interposed postsynaptic spikes could be detected (Figures 6A and 6B). To quantitatively analyze the relation of postsynaptic action potentials to presynaptic spikes at different frequencies, we plotted the postsynaptic action potential firing rate as a function of the presynaptic stimulus number, as shown exemplarily for 20 Hz and 100 Hz stimulus trains in Figure 6C. At both wild-type and Syt7-deficient synapses, presynaptic action potentials were faithfully transmitted as postsynaptic spikes early in the trains, but transmission failures increased later in the train (Figure 6C). In wild-type synapses, transmission failures reached 25% at the end of 20 Hz stimulus trains and 50% at the end of 100 Hz stimulus trains. The Syt7 KO dramatically enhanced the failures during the 100 Hz but not the 20 Hz stimulus trains (Figure 6C). Thus, Syt7-mediated asynchronous release during the stimulus train appears to boost reliable spike transmission at the calyx synapse.

To better characterize the paradoxical increase in synchronous transmission by asynchronous release, we plotted the frequency of postsynaptic action potentials as a function of presynaptic stimulation at 20, 50, 100, and 200 Hz for the entire stimulus train, the initial 5 stimuli, or the last 20 stimuli (Figure 6D). We found that the Syt7 KO had no significant effect on transmission fidelity at 20 or 50 Hz but dramatically decreased transmission fidelity at 100 or 200 Hz. Importantly, the Syt7 KO did not impact transmission for the first 5 presynaptic stimuli but decreased transmission during the last 20 stimuli by >80% (Figure 6D). Thus, Syt7-dependent asynchronous release is selectively required for high-frequency transmission of synchronous synaptic release signals.

A plausible mechanism by which the asynchronous basal current might increase spike transmission fidelity is that the basal current produces partial postsynaptic depolarization throughout the train that then enhances action potential generation. To test this hypothesis, we applied low concentrations (5 μM) of cyclothiazide, which partly inhibits AMPA receptor desensitization and thereby increases the decay times of EPSCs, thus creating the effect of a basal current (Figures S7A–S7C). We then examined whether this artificially induced basal current could rescue the impairment in high-fidelity synaptic transmission in Syt7 KO calyx synapses (Figures 6E–6G). In the presence of 5 μM cyclothiazide, Syt7 KO synapses exhibited fewer transmission failures than control synapses under corresponding conditions without cyclothiazide, suggesting that the partial background depolarization rescued the Syt7 KO phenotype (Figure 6G).

Syt7 Deletion Impairs Temporal Spiking Precision during High-Frequency Stimulation

Information coding at a synapse depends not only on the reliability of synaptic transmission but also on the precision of the temporal association between synaptic inputs and outputs (Trussell, 1999; Xu et al., 2012). Therefore, we further examined whether the Syt7 KO alters the timings of postsynaptic spikes during 20 Hz and 100 Hz stimulus trains. In control mice, the delay of neuronal spiking increased when a neuron fired repetitively (Figures 7A and 7B). During 20 Hz stimulus trains, we observed a progressive increase in spiking latency in wild-type mice even though the fidelity of spike generation remained high, such that almost every synaptic input triggered an action potential (Figure 7C). This increase in spiking latency was aggravated at 100 Hz (Figure 7D). The Syt7 KO significantly enhanced the increase in spiking latency at both 20 Hz and 100 Hz, suggesting that Syt7-mediated asynchronous release enables the high temporal precision of synaptic transmission during action potential trains (Figures 7A–7D; Figure S8). No significant

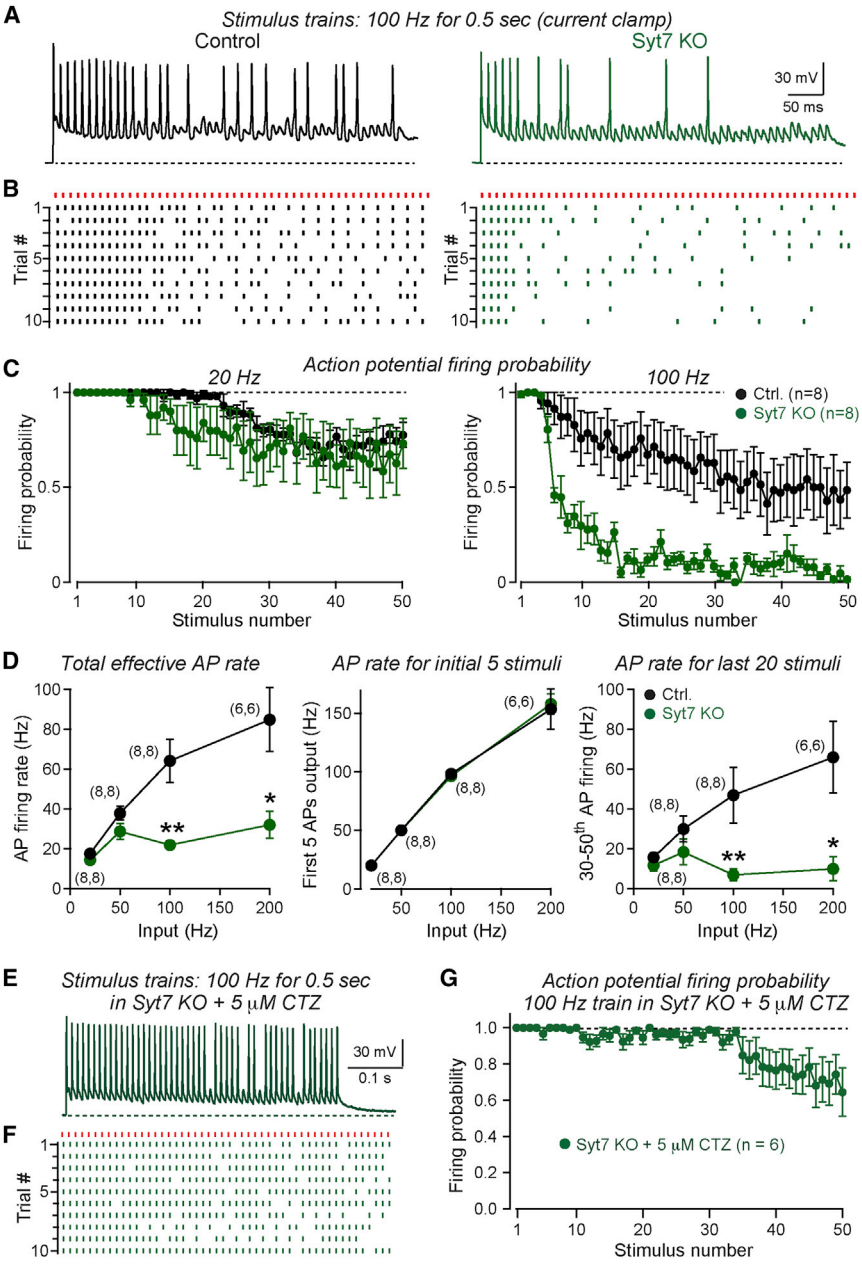

Figure 6. Impaired Asynchronous Release Induced by Syt7 KO Reduces the Reliability of Synaptic Transmission during High-Frequency Stimulation

(A) Example traces of action potentials monitored in patched MNTB neurons in current-clamp mode as a function of high-frequency extracellular fiber stimulation (100 Hz for 0.5 s). EPSPs were recorded from MNTB neurons (held at −70 mV by 20–200 pA current injections) in acute brainstem slices from littermate control and Syt7 KO mice at P11–P14. Similar experiments were performed for frequencies ranging from 20 to 200 Hz.

(B) Representative raster plots of action potential spikes evoked by 100 Hz, 0.5 s stimulus trains repeated with 80 s intervals.

(C) Summary plots of the spiking probability of NMTB neurons as a function of stimulus number in response to presynaptic trains of 50 action potentials induced at 20 Hz (left) or 100 Hz (right).

(D) Summary plots comparing the postsynaptic spike outputs as a function of the presynaptic action potential inputs for stimulation frequencies ranging from 20 to 200 Hz (50 stimuli each). The output rate was determined for the entire stimulus train (left), the first 5 stimuli (middle), and the last 20 stimuli (right).

(E) Example traces of action potentials monitored in Syt7 KO MNTB neurons in current-clamp mode as described for (A) but in the presence of 5 μM cyclothiazide (CTZ).

(F) Representative raster plots of action potential spikes obtained in the experiments described in (E). The synapse was stimulated by afferent fiber stimulation at 100 Hz, 0.5 s; stimulus trains were repeated every 80 s.

(G) Summary plots of the spiking probability of Syt7 KO NMTB neurons as a function of stimulus number in response to presynaptic trains of 50 action potentials induced at 100 Hz in the presence of 5 μM CTZ (compare to C to assess rescue of Syt7 KO phenotype by CTZ).

Data are means ± SEM. Number of analyzed cells (from at least three mice per group) are shown in the graph (C, D, and G); statistical significance was assessed by one-way *ANOVA* with Tukey's post hoc test (*$p < 0.05$; **$p < 0.01$). For additional data, see Figure S7.

changes in the properties of pre- or postsynaptic action potentials were apparent (Figures 7E and 7F). Thus, asynchronous release mediated by Syt7 boosts not only the reliability of synchronous synaptic transmission during repeated action potentials but also the precise timing of individual synaptic responses even at intermediate stimulation frequencies.

Syt7 KO Phenotype Persists in More Mature Calyx Synapses at P15–P16

Owing to the more precise analysis possibilities, our experiments were mostly performed with calyx synapses at P11–P14. However, at that immature stage, the calyx synapse has a lower transmission fidelity than later in development (Taschenberger and von Gersdorff, 2000). To test whether the Syt7 KO phenotype persists in more mature synapses, we analyzed EPSCs induced by 100 Hz stimulus trains in calyx synapses at P15–P16 (Figures 8A–8F; Figure S8F). We observed essentially the same phenotype in Syt7 KO synapses as in less mature synapses, with the only significant Syt7-KO-induced change being an ~80% decrease in the basal current during the train (Figure 8F). We then asked whether this loss of the asynchronous basal current also impairs transmission fidelity in more mature calyx synapses. The Syt7 KO again decreased transmission fidelity late in 100 Hz trains, causing a significant decrease in the effective action potential rate (Figures 8G–8J). Thus, the Syt7 function we delineate here is not restricted to a particular developmental stage.

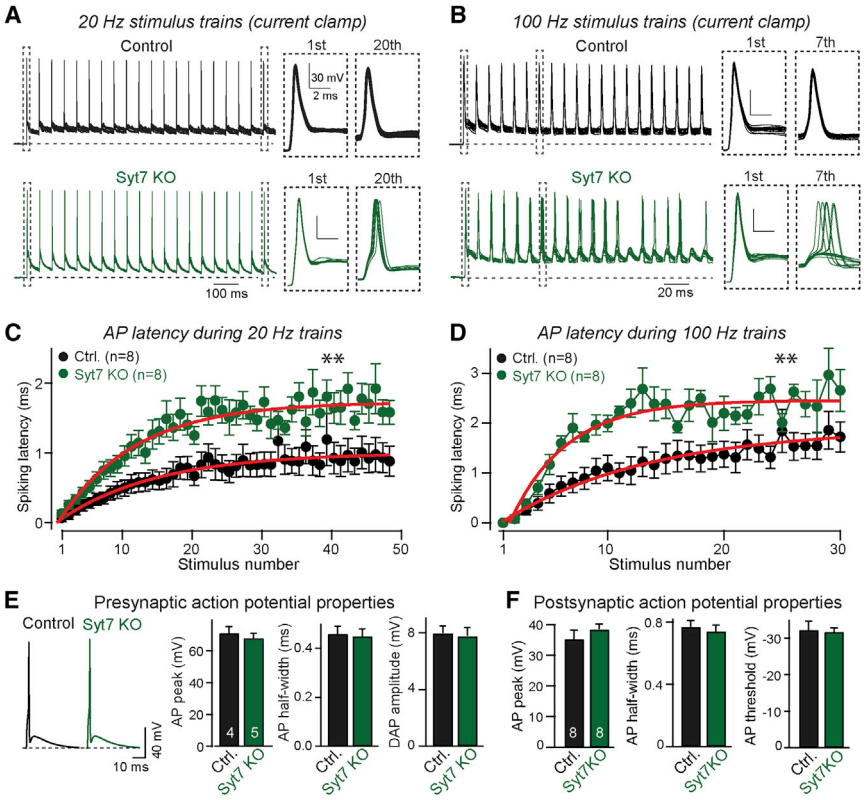

Figure 7. Decrease in Presynaptic Asynchronous Release in Syt7 KO Synapses Impairs the Temporal Precision of Postsynaptic Action Potential Firing

(A and B) Superimposed 10 traces of postsynaptic action potentials induced by trains of 50 presynaptic action potentials evoked at 20 Hz (A) or 100 Hz (B) by extracellular fiber stimulation. Action potentials were recorded in current-clamp mode in MNTB neurons from littermate control and Syt7 KO mice at P11–P14. For clarity, only the first 20 responses are shown. Expansions on the right display the 1st and 20th (A) or 1st and 7th (B) action potentials to illustrate action potential jitters and failures.

(C and D) Summary graphs of the spiking latency (normalized to the 1st action potential), plotted as a function of the stimulus number during 20 Hz (C) or 100 Hz (D) trains.

(E) Presynaptic action potential properties are unchanged in Syt7 KO neurons (left, representative traces; right, summary graphs of the action potential peaks, half-widths, and depolarization-after-potential (DAP) amplitudes).

(F) Postsynaptic action potential properties are also unchanged in Syt7 KO neurons (summary graphs of the action potential peaks, half-widths, and firing thresholds).

Data are means ± SEM. Number of analyzed cells (from at least three mice per group) are shown in the graph (C and D) or indicated in the bars (E and F); statistical significance was assessed by two-way *ANOVA* with Tukey's post hoc test (*$p < 0.05$; **$p < 0.01$) or Student's t test (E and F; no significant differences). For additional data, see Figure S8.

DISCUSSION

Syt7-Dependent Asynchronous Release Produces a Basal Current during High-Frequency Stimulation at Calyx Synapses

Asynchronous release is mediated by a delayed form of Ca^{2+}-triggered synaptic vesicle exocytosis and produces a postsynaptic current that per definition is not time locked to the presynaptic action potential. Some synapses exhibit prominent asynchronous release that generates a delayed postsynaptic current, which continues after a stimulus train ends and produces a long-lasting synaptic signal (Best and Regehr, 2009; Daw et al., 2009; Hefft and Jonas, 2005; Iremonger and Bains, 2007; Südhof, 2013). Such long-lasting signaling exhibited by asynchronous GABA release at synapses from fast-spiking interneurons is thought to provide an efficient computational mechanism of inhibition that prevents widespread epileptiform spiking activity (Manseau et al., 2010). Similarly, long-lasting excitation produced by asynchronous glutamate release may promote prolonged spiking of a postsynaptic neuron in which preserving the temporal precision of action potential timing is not necessary (Iremonger and Bains, 2007). In terms of synaptic computation, asynchronous release at these synapses is thus thought to extend the magnitude and duration of synaptic signals induced by spike bursts.

The well-characterized function of asynchronous release in prolonged synaptic signaling raises the question of whether synapses that mediate fast, reliable synaptic transmission and exhibit no delayed synaptic signaling, such as the calyx of Held, actually utilize asynchronous release, and if so, for what functional purpose? This question is particularly pertinent since Syt7, the major—and possibly only—Ca^{2+} sensor for asynchronous release, is highly expressed in almost all neurons, including neurons lacking a prominent delayed asynchronous signaling mode. As an additional confounding issue, it was recently suggested that Syt7 has a second general function as a Ca^{2+} sensor for short-term plasticity in central synapses (Jackman et al., 2016). Although the observations underlying this suggestion could more parsimoniously be explained by the role of Syt7 as a Ca^{2+} sensor for asynchronous release, such an explanation implies that asynchronous release can assume yet another computational role depending on the synapse type. Thus, testing whether Syt7 functions exclusively as a Ca^{2+} sensor for asynchronous release or performs parallel functions in release both as a Ca^{2+} sensor for asynchronous release and for short-term plasticity requires examining Syt7 function in a central synapse that allows a precise dissection of release and that lacks a delayed signaling mode. In the present study, we have done so by examining the specific function of Syt7 and asynchronous release at the calyx of Held synapse.

Our data show that Syt7-dependent asynchronous release contributes significantly to Ca^{2+}-triggered exocytosis at calyx synapses but in an unexpected manner that is not reflected in the amount of total release under physiological conditions:

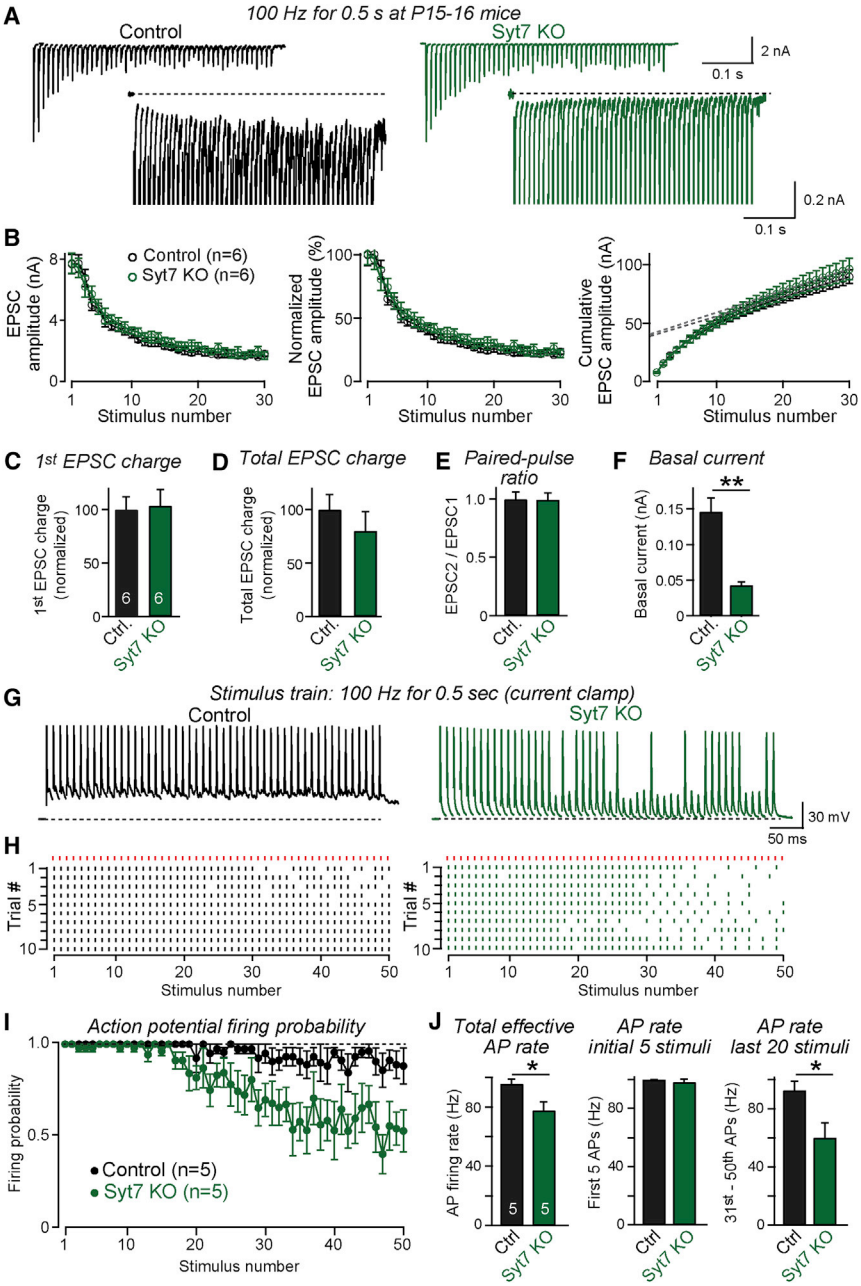

Figure 8. Syt7-Mediated Asynchronous Release Enables Fast Synchronous Synaptic Transmission during High-Frequency Stimulus Trains in More Mature Calyx Synapses at P15–P16

(A) Representative traces of EPSCs evoked by high-frequency trains of extracellular fiber stimulation (100 Hz for 0.5 s) in acute brainstem slices from littermate control and Syt7 KO mice at P15–P16. Expanded traces below full traces illustrate the basal asynchronous EPSC on which synchronous EPSCs ride. Note that Syt7 is selectively required for the basal asynchronous EPSC.

(B) Summary plots of the absolute, normalized, and cumulative EPSC amplitudes plotted against stimulus number. The gray dotted lines in the cumulative EPSC plot illustrate the linear regression fit used to estimate the cumulative EPSC amplitude by back extrapolation to time zero, which corrects for vesicle replenishment during the train.

(C–F) Summary graphs of the normalized synaptic charge transfer during the 1st EPSC (C) or the entire trains (D), the paired-pulse (10 ms interval) ratio of the peak amplitudes of the 2nd and 1st EPSCs (E), and the basal current amplitudes (F), measured as the difference between the sustained currents reached during the train and the baseline (dotted line).

(G) Example traces of action potentials monitored in patched MNTB neurons in current-clamp mode as a function of high-frequency extracellular fiber stimulation (100 Hz for 0.5 s). EPSPs were recorded from MNTB neurons (held at −70 mV by 20–200 pA current injections) in acute brainstem slices from littermate control and Syt7 KO mice at P15–P16.

(H) Representative raster plots of action potential spikes evoked by 100 Hz, 0.5 s stimulus trains repeated with 80 s intervals.

(I) Summary plots of the spiking probability of NMTB neurons as a function of stimulus number in response to presynaptic trains of 50 action potentials induced at 100 Hz.

(J) Summary plots comparing the postsynaptic spike outputs as a function of presynaptic action potential inputs for 50 stimuli at 100 Hz. The output rate was determined for the entire stimulus train (left), the first 5 stimuli (middle), and the last 20 stimuli (right).

Data are means ± SEM. Number of cells (from at least three mice per group) analyzed are shown in the graphs (B and I) or indicated in the bars (C and J); statistical significance was assessed by Student's t test (C–F and J; *p < 0.05; **p < 0.01). For additional data, see Figures S1 and S8.

asynchronous release, activated during stimulus trains, induces a basal postsynaptic current that makes no direct contribution to synchronous postsynaptic currents but causes a continuous incremental postsynaptic depolarization, which in turn enables fast triggering of postsynaptic action potentials that are time locked with presynaptic synchronous release. In this manner, asynchronous release paradoxically boosts the functional efficacy of synchronous release. We present multiple lines of evidence that the basal Syt7-dependent current during high-frequency stimulus trains does in fact represent asynchronous release that can be summarized as follows. First, the basal current is blocked by EGTA-AM. Second, capacitance measurements show that Syt7 mediates a slow form of exocytosis in presynaptic calyx terminals. Third, the Syt7 KO does not change the amplitude of synchronous EPSCs and steady-state EPSCs during prolonged stimulus trains; if Syt7 was involved in Ca^{2+}-dependent vesicle priming as suggested (Liu et al., 2014), these two parameters should have been impaired. Fourth, other

causes of the basal currents, such as a change in EPSC kinetics, were ruled out.

Importantly, our results show that Syt7 does not perform a general function as a Ca^{2+} sensor for short-term plasticity under physiological conditions (Figure 1). However, when Syt2 was deleted and only synchronous release mediated by lower levels of Syt1 remained, the residual synchronous release at the calyx synapse exhibited synaptic facilitation, which was decreased by additional deletion of Syt7 (Figure 4). This result indicates that the activity ratio of fast versus slow synaptotagmin Ca^{2+} sensors dictates whether or not facilitation is observed at the calyx synapse and possibly other synapses. It suggests that Syt7 is not a specific Ca^{2+} sensor for synaptic facilitation but that Syt7 can win the competition with fast Ca^{2+} sensors when the levels of the fast Ca^{2+} sensors are decreased, resulting in a significant contribution of the Syt7-dependent slower Ca^{2+} triggering of release already during the second of two action potentials in a train and thus creating the properties of a Ca^{2+} sensor for synaptic facilitation.

The Syt7-Dependent Basal Current Mediated by Asynchronous Release Boosts Transmission Fidelity at Calyx Synapses

Our arguably most important finding is the unexpected function of asynchronous release at calyx synapses in boosting synchronous synaptic transmission, during which pre- and postsynaptic action potentials are time locked and coupled. We showed that loss of Syt7-dependent asynchronous release in otherwise wild-type synapses with a full complement of synchronous synaptotagmin Ca^{2+} sensors results in a selective decrease in a basal asynchronous postsynaptic current that is induced by a stimulus train and on which the individual synchronous postsynaptic currents ride (Figure 5). This basal postsynaptic current contributes a quantitatively minor component to the total synaptic charge transfer but nevertheless has a crucial function in maintaining reliable synchronous synaptic transmission (Figure 6). The Syt7 deletion that impairs the basal postsynaptic current also decreases the fidelity of postsynaptic action potential generation by presynaptic action potentials during the later stages of a stimulus train, with an almost complete loss in action potential firing after 30 presynaptic spikes (Figure 6). Moreover, the Syt7 deletion renders action potentials less precise, as reflected in a doubling of the apparent spiking latency (Figure 7). These findings define a novel computational function for asynchronous release, namely to enable synchronous synaptic transmission at high rates during extended stimulus trains. At present, we do not know whether the function of asynchronous release in boosting synchronous synaptic transmission is generally applicable. Given the faithful transmission of high-frequency spikes at many synapses in the brain, however, it seems likely that this function is not specific for the calyx synapse.

Diverse Manifestations of Asynchronous Release in Different Synapses

Viewed together, our results suggest that the contribution of Syt7-mediated asynchronous release to synaptic transmission can manifest in at least three ways: (1) as the classical asynchronous release observed as a delayed postsynaptic current after an action potential burst or train (Hefft and Jonas, 2005; Iremonger and Bains, 2007; Daw et al., 2009, 2010); (2) as an increase in the amount of release during short-term plasticity, creating the appearance of a Ca^{2+} sensor for short-term facilitation (Jackman et al., 2016; see also Figure 4); and (3) as a basal postsynaptic current during stimulus bursts and trains that functions to render high-frequency synaptic transmission more precise and reliable (this study).

How does the interplay between fast (Syt1, Syt2, and Syt9) and slow (Syt7) synaptotagmin Ca^{2+} sensors lead to different manifestations of asynchronous release in different synapses? Under all conditions, fast synchronous release mediated by Syt1, Syt2, or Syt9 is responsible for the bulk of the total release, but the activity ratio between them likely dictates their relative contribution. This parsimonious hypothesis suggests that a difference in the relative efficacy of Syt1, Sty2, and Sty9 versus Syt7, either owing to different expression levels or to differential regulation (e.g., phosphorylation; de Jong et al., 2016; Wu et al., 2015), controls the synaptic manifestation of asynchronous release.

This hypothesis posits that under all conditions, Syt1, Syt2, and Syt9 are activated by Ca^{2+} faster than Syt7 and outcompete Syt7, independent of their relative activities. Under "standard" conditions, Syt1, Syt2, and Syt9 mediate nearly all release as synchronous release during low-frequency stimulation or in the beginning of a stimulus train, while Syt7 increasingly contributes an asynchronous component during bursts or trains of action potentials (Maximov and Südhof, 2005). The Syt7-dependent asynchronous component grows in magnitude during the stimulus train as residual Ca^{2+} builds up and activates Syt7; as a result, Syt7 accounts for an increasing component during the train. When the train ends, the prolonged action of Syt7 due to slowly decaying residual Ca^{2+} causes a delayed component in some synapses. If Syt1 and Syt2 are much more active than Syt7 under standard conditions, however, Syt7-dependent release only induces an asynchronous postsynaptic current during a stimulus train without influencing short-term synaptic plasticity (which is governed by other Ca^{2+} sensors, such as Munc13-1 or Munc13-2; Junge et al., 2004; Shin et al., 2010; Chen et al., 2013). As a result, Syt7 increases the nonsynchronous postsynaptic current during action potential trains and thereby enhances the reliability and fidelity of synchronous synaptic transmission. If Syt1 and Syt2 are relatively less active compared to Syt7, however, Syt7-induced release already kicks in during the second action potential and facilitates the response, creating the impression that Syt7 is a Ca^{2+} sensor for short-term plasticity.

Future Perspectives

Not surprisingly, our results raise many new questions. Most pressing among these questions is probably the issue of the number of different Ca^{2+} sensors for release: how many Ca^{2+} sensors are there, and how do Syt1-, Syt2-, and Syt9-dependent synchronous and Syt7-dependent asynchronous release relate to the types of release characterized by Sun et al. (2007)? Note that some of the slow phase of Ca^{2+}-triggered exocytosis, as measured by capacitance, persists even in the absence of Syt2 or Syt7 (Figure 3); this phase probably corresponds to the release mediated by the second Ca^{2+} sensor of Sun et al.

(2007) and does not constitute classical asynchronous release. Thus, synapses likely express two classes of Ca^{2+} sensors, different synaptotagmins with a distinct kinetics that mediate synchronous and asynchronous release and another type of Ca^{2+}-binding protein whose function as a Ca^{2+} sensor for release is normally occluded by synaptotagmins. According to this hypothesis, the function of the second type of Ca^{2+}-binding protein in release becomes apparent only when fast synaptotagmins are deleted and manifests as increased spontaneous mini release and as delayed evoked release that is even slower than Syt7-mediated asynchronous release (Sun et al., 2007; Xu et al., 2009). Although the nature of the second class of Ca^{2+} sensors remains unclear, an attractive candidate is Munc13. The priming function of Munc13 is Ca^{2+} activated; via this activation, Munc13 could serve as an apparent Ca^{2+} sensor for exocytosis, even though its normal Ca^{2+}-regulated function is priming (Junge et al., 2004; Shin et al., 2010). Testing this hypothesis will require even more complex mouse models than currently available but will hopefully be achievable in future.

STAR★METHODS

Detailed methods are provided in the online version of this paper and include the following:

- KEY RESOURCES TABLE
- CONTACT FOR REAGENT AND RESOURCE SHARING
- EXPERIMENTAL MODEL AND SUBJECT DETAILS
  - Animals
  - Generation of Syt2 cKO mice and mouse breeding
  - Deletion of Syt2 at the calyx of Held synapse in Syt2 cKO/PV^{Cre} and Syt2 cKO/PV^{Cre}/Syt7 KO mice
- METHOD DETAILS
  - Preparation of acute slices for electrophysiology
  - Postsynaptic voltage-clamp recordings
  - Postsynaptic current-clamp recordings
  - Presynaptic capacitance measurement
  - Presynaptic current-clamp recordings
  - Immunohistochemistry
  - Quantifications and statistical analyses

SUPPLEMENTAL INFORMATION

Supplemental Information includes eight figures and can be found with this article online at http://dx.doi.org/10.1016/j.neuron.2017.04.020.

AUTHOR CONTRIBUTIONS

F.L. performed all experiments for the current study; F.L. and T.C.S. planned the experiments, analyzed the data, and wrote the manuscript.

ACKNOWLEDGMENTS

We thank Dr. Z. Pang, Dr. T. Bacaj, and Dr. W. Xu for the initial generation of conditional Syt2 KO mice. This study was supported by NIH grant MH086403.

Received: November 12, 2016
Revised: March 31, 2017
Accepted: April 13, 2017
Published: May 17, 2017

REFERENCES

Bacaj, T., Wu, D., Yang, X., Morishita, W., Zhou, P., Xu, W., Malenka, R.C., and Südhof, T.C. (2013). Synaptotagmin-1 and synaptotagmin-7 trigger synchronous and asynchronous phases of neurotransmitter release. Neuron *80*, 947–959.

Baydyuk, M., Xu, J., and Wu, L.G. (2016). The calyx of Held in the auditory system: structure, function, and development. Hear. Res. *338*, 22–31.

Best, A.R., and Regehr, W.G. (2009). Inhibitory regulation of electrically coupled neurons in the inferior olive is mediated by asynchronous release of GABA. Neuron *62*, 555–565.

Borst, J.G., and Sakmann, B. (1996). Calcium influx and transmitter release in a fast CNS synapse. Nature *383*, 431–434.

Chen, Z., Cooper, B., Kalla, S., Varoqueaux, F., and Young, S.M., Jr. (2013). The Munc13 proteins differentially regulate readily releasable pool dynamics and calcium-dependent recovery at a central synapse. J. Neurosci. *33*, 8336–8351.

Crawford, D.C., and Kavalali, E.T. (2015). Molecular underpinnings of synaptic vesicle pool heterogeneity. Traffic *16*, 338–364.

Daw, M.I., Tricoire, L., Erdelyi, F., Szabo, G., and McBain, C.J. (2009). Asynchronous transmitter release from cholecystokinin-containing inhibitory interneurons is widespread and target-cell independent. J. Neurosci. *29*, 11112–11122.

Daw, M.I., Pelkey, K.A., Chittajallu, R., and McBain, C.J. (2010). Presynaptic kainate receptor activation preserves asynchronous GABA release despite the reduction in synchronous release from hippocampal cholecystokinin interneurons. J. Neurosci. *30*, 11202–11209.

de Jong, A.P., Meijer, M., Saarloos, I., Cornelisse, L.N., Toonen, R.F., Sørensen, J.B., and Verhage, M. (2016). Phosphorylation of synaptotagmin-1 controls a post-priming step in PKC-dependent presynaptic plasticity. Proc. Natl. Acad. Sci. USA *113*, 5095–5100.

Evstratova, A., Chamberland, S., Faundez, V., and Tóth, K. (2014). Vesicles derived via AP-3-dependent recycling contribute to asynchronous release and influence information transfer. Nat. Commun. *5*, 5530.

Felmy, F., and Schneggenburger, R. (2004). Developmental expression of the Ca2+-binding proteins calretinin and parvalbumin at the calyx of Held of rats and mice. Eur. J. Neurosci. *20*, 1473–1482.

Forsythe, I.D. (1994). Direct patch recording from identified presynaptic terminals mediating glutamatergic EPSCs in the rat CNS, in vitro. J. Physiol. *479*, 381–387.

Geppert, M., Goda, Y., Hammer, R.E., Li, C., Rosahl, T.W., Stevens, C.F., and Südhof, T.C. (1994). Synaptotagmin I: a major Ca^{2+} sensor for transmitter release at a central synapse. Cell *79*, 717–727.

Goda, Y., and Stevens, C.F. (1994). Two components of transmitter release at a central synapse. Proc. Natl. Acad. Sci. USA *91*, 12942–12946.

Hagler, D.J., Jr., and Goda, Y. (2001). Properties of synchronous and asynchronous release during pulse train depression in cultured hippocampal neurons. J. Neurophysiol. *85*, 2324–2334.

Hefft, S., and Jonas, P. (2005). Asynchronous GABA release generates long-lasting inhibition at a hippocampal interneuron-principal neuron synapse. Nat. Neurosci. *8*, 1319–1328.

Iremonger, K.J., and Bains, J.S. (2007). Integration of asynchronously released quanta prolongs the postsynaptic spike window. J. Neurosci. *27*, 6684–6691.

Jackman, S.L., Turecek, J., Belinsky, J.E., and Regehr, W.G. (2016). The calcium sensor synaptotagmin 7 is required for synaptic facilitation. Nature *529*, 88–91.

Junge, H.J., Rhee, J.S., Jahn, O., Varoqueaux, F., Spiess, J., Waxham, M.N., Rosenmund, C., and Brose, N. (2004). Calmodulin and Munc13 form a Ca^{2+} sensor/effector complex that controls short-term synaptic plasticity. Cell *118*, 389–401.

Kaeser, P.S., and Regehr, W.G. (2014). Molecular mechanisms for synchronous, asynchronous, and spontaneous neurotransmitter release. Annu. Rev. Physiol. *76*, 333–363.

Kochubey, O., and Schneggenburger, R. (2011). Synaptotagmin increases the dynamic range of synapses by driving Ca^{2+}-evoked release and by clamping a near-linear remaining Ca^{2+} sensor. Neuron *69*, 736–748.

Kochubey, O., Babai, N., and Schneggenburger, R. (2016). A synaptotagmin isoform switch during the development of an identified CNS synapse. Neuron *90*, 984–999.

Lindau, M., and Neher, E. (1988). Patch-clamp techniques for time-resolved capacitance measurements in single cells. Pflugers Arch. *411*, 137–146.

Liu, H., Bai, H., Hui, E., Yang, L., Evans, C.S., Wang, Z., Kwon, S.E., and Chapman, E.R. (2014). Synaptotagmin 7 functions as a Ca^{2+}-sensor for synaptic vesicle replenishment. eLife *3*, e01524.

Lorteije, J.A., Rusu, S.I., Kushmerick, C., and Borst, J.G. (2009). Reliability and precision of the mouse calyx of Held synapse. J. Neurosci. *29*, 13770–13784.

Luo, F., Bacaj, T., and Südhof, T.C. (2015). Synaptotagmin-7 is essential for Ca^{2+}-triggered delayed asynchronous release but not for Ca^{2+}-dependent vesicle priming in retinal ribbon synapses. J. Neurosci. *35*, 11024–11033.

Manseau, F., Marinelli, S., Méndez, P., Schwaller, B., Prince, D.A., Huguenard, J.R., and Bacci, A. (2010). Desynchronization of neocortical networks by asynchronous release of GABA at autaptic and synaptic contacts from fast-spiking interneurons. PLoS Biol. *8*, e1000492.

Maximov, A., and Südhof, T.C. (2005). Autonomous function of synaptotagmin 1 in triggering synchronous release independent of asynchronous release. Neuron *48*, 547–554.

Maximov, A., Lao, Y., Li, H., Chen, X., Rizo, J., Sørensen, J.B., and Südhof, T.C. (2008). Genetic analysis of synaptotagmin-7 function in synaptic vesicle exocytosis. Proc. Natl. Acad. Sci. USA *105*, 3986–3991.

Mc Laughlin, M., van der Heijden, M., and Joris, P.X. (2008). How secure is in vivo synaptic transmission at the calyx of Held? J. Neurosci. *28*, 10206–10219.

Otsu, Y., Shahrezaei, V., Li, B., Raymond, L.A., Delaney, K.R., and Murphy, T.H. (2004). Competition between phasic and asynchronous release for recovered synaptic vesicles at developing hippocampal autaptic synapses. J. Neurosci. *24*, 420–433.

Pang, Z.P., Melicoff, E., Padgett, D., Liu, Y., Teich, A.F., Dickey, B.F., Lin, W., Adachi, R., and Südhof, T.C. (2006a). Synaptotagmin-2 is essential for survival and contributes to Ca^{2+} triggering of neurotransmitter release in central and neuromuscular synapses. J. Neurosci. *26*, 13493–13504.

Pang, Z.P., Sun, J., Rizo, J., Maximov, A., and Südhof, T.C. (2006b). Genetic analysis of synaptotagmin 2 in spontaneous and Ca^{2+}-triggered neurotransmitter release. EMBO J. *25*, 2039–2050.

Schonn, J.S., Maximov, A., Lao, Y., Südhof, T.C., and Sørensen, J.B. (2008). Synaptotagmin-1 and -7 are functionally overlapping Ca^{2+} sensors for exocytosis in adrenal chromaffin cells. Proc. Natl. Acad. Sci. USA *105*, 3998–4003.

Shin, O.-H., Lu, J., Rhee, J.-S., Tomchick, D.R., Pang, Z.P., Wojcik, S.M., Camacho-Perez, M., Brose, N., Machius, M., Rizo, J., et al. (2010). Munc13 C_2B domain is an activity-dependent Ca^{2+} regulator of synaptic exocytosis. Nat. Struct. Mol. Biol. *17*, 280–288.

Stevens, C.F. (2003). Neurotransmitter release at central synapses. Neuron *40*, 381–388.

Südhof, T.C. (2013). Neurotransmitter release: the last millisecond in the life of a synaptic vesicle. Neuron *80*, 675–690.

Sugita, S., Han, W., Butz, S., Liu, X., Fernández-Chacón, R., Lao, Y., and Südhof, T.C. (2001). Synaptotagmin VII as a plasma membrane $Ca^{(2+)}$ sensor in exocytosis. Neuron *30*, 459–473.

Sugita, S., Shin, O.-H., Han, W., Lao, Y., and Südhof, T.C. (2002). Synaptotagmins form a hierarchy of exocytotic $Ca^{(2+)}$ sensors with distinct $Ca^{(2+)}$ affinities. EMBO J. *21*, 270–280.

Sun, J.Y., and Wu, L.G. (2001). Fast kinetics of exocytosis revealed by simultaneous measurements of presynaptic capacitance and postsynaptic currents at a central synapse. Neuron *30*, 171–182.

Sun, J., Pang, Z.P., Qin, D., Fahim, A.T., Adachi, R., and Südhof, T.C. (2007). A dual-Ca^{2+}-sensor model for neurotransmitter release in a central synapse. Nature *450*, 676–682.

Takahashi, T. (2015). Strength and precision of neurotransmission at mammalian presynaptic terminals. Proc. Jpn. Acad., Ser. B, Phys. Biol. Sci. *91*, 305–320.

Taschenberger, H., and von Gersdorff, H. (2000). Fine-tuning an auditory synapse for speed and fidelity: developmental changes in presynaptic waveform, EPSC kinetics, and synaptic plasticity. J. Neurosci. *20*, 9162–9173.

Trussell, L.O. (1999). Synaptic mechanisms for coding timing in auditory neurons. Annu. Rev. Physiol. *61*, 477–496.

Walter, A.M., Groffen, A.J., Sørensen, J.B., and Verhage, M. (2011). Multiple Ca^{2+} sensors in secretion: teammates, competitors or autocrats? Trends Neurosci. *34*, 487–497.

Wang, L.Y., and Augustine, G.J. (2015). Presynaptic nanodomains: a tale of two synapses. Front. Cell. Neurosci. *8*, 455.

Wen, H., Linhoff, M.W., McGinley, M.J., Li, G.L., Corson, G.M., Mandel, G., and Brehm, P. (2010). Distinct roles for two synaptotagmin isoforms in synchronous and asynchronous transmitter release at zebrafish neuromuscular junction. Proc. Natl. Acad. Sci. USA *107*, 13906–13911.

Wu, B., Wei, S., Petersen, N., Ali, Y., Wang, X., Bacaj, T., Rorsman, P., Hong, W., Südhof, T.C., and Han, W. (2015). Synaptotagmin-7 phosphorylation mediates GLP-1-dependent potentiation of insulin secretion from β-cells. Proc. Natl. Acad. Sci. USA *112*, 9996–10001.

Xu, J., Mashimo, T., and Südhof, T.C. (2007). Synaptotagmin-1, -2, and -9: $Ca^{(2+)}$ sensors for fast release that specify distinct presynaptic properties in subsets of neurons. Neuron *54*, 567–581.

Xu, J., Pang, Z.P., Shin, O.H., and Südhof, T.C. (2009). Synaptotagmin-1 functions as a Ca^{2+} sensor for spontaneous release. Nat. Neurosci. *12*, 759–766.

Xu, W., Morishita, W., Buckmaster, P.S., Pang, Z.P., Malenka, R.C., and Südhof, T.C. (2012). Distinct neuronal coding schemes in memory revealed by selective erasure of fast synchronous synaptic transmission. Neuron *73*, 990–1001.

Yoshihara, M., and Littleton, J.T. (2002). Synaptotagmin I functions as a calcium sensor to synchronize neurotransmitter release. Neuron *36*, 897–908.

Zhang, B., Seigneur, E., Wei, P., Gokce, O., Morgan, J., and Südhof, T.C. (2016). Developmental plasticity shapes synaptic phenotypes of autism-associated neuroligin-3 mutations in the calyx of Held. Mol. Psychiatry. http://dx.doi.org/10.1038/mp.2016.157.

STAR★METHODS

KEY RESOURCES TABLE

REAGENT or RESOURCE	SOURCE	IDENTIFIER
Antibodies		
Rabbit polyclonal anti-syt2	Pang et al., 2006a	RRID: AB_2650431
Guinea pig polyclonal anti-VGluT1	Millipore	Cat#:AB5905; RRID: AB_2301751
Experimental Models: Organisms/Strains		
Mouse, Syt2 cKO (B6;129S6-Syt2^{tm2Sud}/J)	This paper	JAX: 023400 RRID: IMSR_JAX:023400
Mouse, Syt7 KO (Syt7^{tm2Sud})	JAX	JAX: 006389; RRID: IMSR_JAX:006389
Mouse, PV-Cre (Pvalb$^{tm1(cre)Arbr}$)	JAX	JAX: 017320 RRID: IMSR_JAX:017320
Oligonucleotides		
S70113: CAG GTG CTG AGG CTT ATC ACA GCA GG	IDT	N/A
S70197: TGG GAG CTG GCT GCA TGC TTT TTA AGT GGG TG	IDT	N/A
S70111: GGC TGC AGG AAT TCG ATA TCA AGC TT	IDT	N/A
S2C079: CTG AGC GCA TGC TGA CAT GT	IDT	N/A
S2C080: AGC TTT CCT GGT GCT GAA AG	IDT	N/A
S2C091: TTA TAC GAA GTT ATT CGA GGT CGA ATC GAT C	IDT	N/A
S2C092: GTA TCT GTC CTT CAG TCT CTC CTG G	IDT	N/A
CRE031: CAC CCT GTT ACG TAT AGC CG	IDT	N/A
CRE032: GAG TCA TCC TTA GCG CCG TA	IDT	N/A
Software and Algorithms		
Element analysis Nikon	Nikon	https://www.nikoninstruments.com/Products/Software; SCR_014329
miniAnalysis	Synaptosoft	http://www.synaptosoft.com/MiniAnalysis/
Igor Pro	WaveMetrics	https://www.wavemetrics.com/products/igorpro/igorpro.htm

CONTACT FOR REAGENT AND RESOURCE SHARING

Further information and requests for resources and reagents should be directed to and will be fulfilled by the Lead Contact, Thomas C. Südhof (tcs1@stanford.edu).

EXPERIMENTAL MODEL AND SUBJECT DETAILS

Animals

All experiments were approved by the Institutional Animal Care and Use Committee at Stanford University. KO and control (including wild-type and heterozygous) littermates of either sex were used. No statistical tests were used to predetermine sample size. All electrophysiology experiments except those involving CTZ (Figures 6E–6G; Figures S7A–S7C) were performed with anonymized sample in which the experimenter was unaware of the experimental condition of a neuron.

Generation of Syt2 cKO mice and mouse breeding

Syt2 cKO (Syt2$^{f/f}$) mice were generated using standard homologous recombination (Geppert et al., 1994). Details of the homologous recombination strategy used were shown in Figures 2A and S1. In brief, exon 2 of the wild-type Syt2 gene encoding the transmembrane region was flanked with LoxP recombination sites by homologous recombination in embryonic stem cells to generate Syt2 cKO mice. We crossed the conditional Syt2$^{f/f}$ and the constitutive Syt7$^{-/-}$ mice (Maximov et al., 2008) to produce different colonies of Syt2$^{f/f}$/Syt7$^{-/-}$ and Syt2$^{f/f}$/Syt7$^{+/-}$ mice, which were further crossed to produce the mice for analysis of Syt7 KO in synaptic transmission at the calyx of Held (Figure S1D).

Deletion of Syt2 at the calyx of Held synapse in Syt2 cKO/PV^{Cre} and Syt2 cKO/PV^{Cre}/Syt7 KO mice

To specifically delete Syt2 from the calyx of Held synapse, we crossed Syt2$^{f/f}$/Syt7$^{-/-}$ mice to a tissue-specific Cre line, PV^{Cre}, that expresses Cre recombinase under the control of the parvalbumin promoter (Figure S1D). PV-Cre has been shown to turn on at the calyx terminals during early postnatal stage (~P4) (Zhang et al., 2016). We confirmed that under our experimental conditions PV-Cre was able to drive Cre expression and thus delete Syt2 expression in the anterior ventral cochlear nucleus neurons which project the calyx of Held terminals to the MNTB neurons (Figure 2A). We used the following combination of oligonucleotide primers for genotyping.

Primer Name	Primer Sequence	PCR Product Size (bp)	Description
S2C079	CTG AGC GCA TGC TGA CAT GT	201	WT
S2C080	AGC TTT CCT GGT GCT GAA AG		
S2C091	TTA TAC GAA GTT ATT CGA GGT CGA ATC GAT C	283	Mutant
S2C092	GTA TCT GTC CTT CAG TCT CTC CTG G		
S70111	GGC TGC AGG AAT TCG ATA TCA AGC TT	380	Mutant
S70113	CAG GTG CTG AGG CTT ATC ACA GCA GG		
S70113	CAG GTG CTG AGG CTT ATC ACA GCA GG	400	WT
S70197	TGG GAG CTG GCT GCA TGC TTT TTA AGT GGG TG		
Cre1301	CAC CCT GTT ACG TAT AGC CG	350	Mutant
Cre1302	GAG TCA TCC TTA GCG CCG TA		

METHOD DETAILS

Preparation of acute slices for electrophysiology

Transverse brain slices containing the MNTB nucleus were prepared from postnatal day 11-16 mice of various transgenic alleles as described (Sun et al., 2007). P15-16 mice were used for studying more mature synapses. Specifically, 200 μm slices (for P11-14 mice) or 150 μm slices (for P15-16 mice) were cut using a Vibratome (VT1200s; Leica) in oxygenated ACSF containing the following (in mM): 119 NaCl, 26 $NaHCO_3$, 10 glucose, 1.25 NaH_2PO_4, 2.5 KCl, 2 $CaCl_2$, 1 $MgCl_2$, 2 Na-pyruvate, and 0.5 ascorbic acid, pH 7.4. After incubation at 35°C for 45 min, slices were stored at room temperature (~21-23°C) for experiments.

Postsynaptic voltage-clamp recordings

All patch-clamp recording were made with the EPC 10 amplifier (HEKA, Lambrecht, Germany). Whole-cell voltage-clamp recordings were made from principal cells in the MNTB visualized by infrared differential interference contrast (IR-DIC) video microscopy (Axioskop 2; Zeiss). Patch pipettes (resistance of 3–4 MΩ) were pulled using borosilicate glass (WPI) on a two-stage vertical puller (Narishige). Series resistances (< 12 MΩ) were compensated by 70%–90% in order to maintain a residual resistance of < 2 MΩ. Cells were voltage-clamped at −70 mV, and EPSCs were recorded in ACSF containing picrotoxin (100 μM), strychnine (2 μM), and D-AP5 (50 μM) to block $GABA_A$ receptors, glycine receptors, and NMDA receptors, respectively. The pipette internal solution contained (in mM): 120 Cs-gluconate, 20 tetraethylammonium-Cl, 20 HEPES, 2 EGTA, 4 MgATP, 0.4 NaGTP, 10 phosphocreatine, and 2 Qx-314. EPSCs were evoked by afferent fiber stimulation (0.1-0.5 mA, 0.1 ms) with a bipolar electrode positioned halfway between mideline and the MNTB to ensure that the calyx was activated in an all-or-none manner. For recordings of mEPSCs, tetrodotoxin (TTX, 0.5 μM) was added to the ACSF.

Postsynaptic current-clamp recordings

Whole-cell current-clamped recordings were performed similar to voltage-clamp recordings, except that the internal solution used contained (in mM): 120 K-gluconate, 20 HEPES, 1 EGTA, 4 MgATP, 0.4 NaGTP, and 10 phosphocreatine, 310-320 mOsmol, pH 7.2. The membrane potential was maintained at approximately −70 mV with current injections of < 200 pA. EPSPs and action potentials were evoked by afferent fiber stimulation (0.1-0.5 mA, 0.1 ms) with a bipolar electrode positioned halfway between mideline and the MNTB to ensure the calyx was activated in an all-or-none manner.

Presynaptic capacitance measurement

To measure exocytosis directly from the presynaptic terminal, we patched the calyx terminal and maintained it in whole-cell voltage-clamp mode (Sun and Wu, 2001). Capacitance measurements were made with the EPC 10 amplifier (HEKA, Lambrecht, Germany) with the lock-in software in PatchMaster (HEKA, Lambrecht, Germany). The sinusoidal stimulus frequency was 1,000 Hz with a peak-to-peak voltage less than 60 mV. We routinely held the cell membrane potential at −80 mV. To induce Ca^{2+} influx and synaptic vesicle fusion, we depolarized the cell from the holding membrane potential to +10 mV for 20 ms or 50 ms. During depolarizations, the

capacitance was not measured. The stimulus-evoked capacitance jump was calculated as the capacitance difference by subtracting the baseline, as averaged 5 s before stimulation, from the capacitance value after stimulation. Fast capacitance jump and maximum capacitance were measured as the value immediately after stimulation or as the peak value (before the capacitance started to decline again owing to endocytosis), respectively. Ca^{2+} currents were pharmacologically isolated with a bath solution containing (in mM): 105 NaCl, 20 TEA-Cl, 2.5 KCl, 1 $MgCl_2$, 2 $CaCl_2$, 25 $NaHCO_3$, 1.25 NaH_2PO_4, 25 glucose, 0.4 ascorbic acid, 3 myo-inositol, 2 Na-pyruvate, 0.001 tetrodotoxin (TTX), 0.1 3,4-diaminopyridine, 300–310 mOsm, pH 7.4 when bubbled with 95% O2 and 5% CO2. The pipette contained (in mM): 125 Cs-gluconate, 20 CsCl, 4 MgATP, 10 Na2-phosphocreatine, 0.3 GTP, 10 HEPES, 0.05 BAPTA, 310–320 mOsm, pH 7.2 adjusted with CsOH. Patch pipettes (resistance of 3–4 MΩ) were used and series resistances (< 20 MΩ) were compensated by 70%–90%.

Presynaptic current-clamp recordings

In one set of experiments, whole cell current-clamp recordings of the calyx were made to measure the presynaptic action potential waveforms. The patch-pipette internal solution contained (in mM): 140 K-gluconate, 20 KCl, 10 HEPES, 0.05 BAPTA, 4 ATP-Magnesium, 0.4 GTP-Sodium, 10 Na-Phosphocreatine, 310-320 mOsmol, pH 7.2 adjusted with KOH. Single action potentials were triggered by injecting short 1 ms current of 0.5 nA trough the pipette. The external solution was the same as in the current-clamp postsynaptic recordings.

Immunohistochemistry

Animals were anesthetized and perfused with 1x PBS for 5 min followed by 5 min 4% paraformaldehyde (PFA). The brains were isolated and fixed in 4% PFA overnight. The tissues were then incubated in 30% sucrose 48 hr for cryo-protection. Brain sections of 30 μm were cut on a cryostat (CM3050S, Leica). The slices were pretreated with 0.5% Triton X-100 for 1 hr at room temperature and incubated overnight at 4°C with primary antibodies in blocking solution (0.1% Triton X-100 and 5% goat serum in PBS). The slices were washed and incubated with fluorescence-conjugated secondary antibodies for 2 hr at room temperature. The slices were washed and mounted with DAPI fluoromount (SouthernBiotech). Primary antibodies against Syt2 (rabbit, polyclonal, 1:1000, A320) and VGluT1 (guinea pig, polyclonal, 1:1000, Millipore) were used. Secondary antibodies were Alexa Fluor conjugates (1:500; Invitrogen). Images were acquired using Nikon A1RSi confocal microscope with a 60 × oil-immersion objective (1.45 numerical aperture) and analyzed in Nikon Analysis software.

Quantifications and statistical analyses

Data were acquired using PatchMaster (EPC 10, HEKA Elektronik) and analyzed in Igor Pro (Wavemetrics). Spontaneous and miniature synaptic currents were detected (threshold = 8 pA) and analyzed in MiniAnalysis (Synaptosoft). For clarity, all stimulus artifacts were blanked and are not showed in the figures. All data are shown as means ± SEM. The numbers of analyzed cells from at least 2 mice per group were shown in the graph as indicated in the figures. One-way or two-way ANOVA tests were performed for statistics of multiple-group comparisons and repetitive measurements; Student's t test was used for two-group comparisons. Statistical significance was defined and indicated in the figures and figure legends as follows: *, $p < 0.05$; **, $p < 0.01$; ***, $p < 0.001$.